Measurement of displacement using double collimators and variable spacing grating fabricated by electron beam lithography

WEI HE[1,2,*], QIMENG TAN[3,*], YUNHUI DONG[1,2], ZHIHAN LI[1,2], LIANQING ZHU[1,2]
[1]*Key Laboratory of the Ministry of Education for Optoelectronic Measurement Technology and Instrument, Beijing Information Science & Technology University, Beijing 100192, China*
[2]*Beijing Laboratory of Optical Fiber Sensing and System, Beijing Information Science & Technology University, Beijing 100192, China*
[3]*Beijing Key Laboratory of Intelligent Space Robotic Systems Technology and Applications, Beijing Institute of Spacecraft System Engineering, Beijing 100094, China*

In this study, a displacement sensing system based on a variable spacing grating was proposed and experimentally demonstrated. The variable spacing grating was fabricated by electron beam lithography and reactive ion etching technique, and the initial line density was 950 L/mm. Double collimators were selected for transmit incident light and receive diffracted light respectively, and the incident and diffracted light angles were maintained at 46°. A one-dimensional displacement platform was controlled to move the light spot on the grating surface, during 40 mm displacement, the central wavelength of the diffraction spectra was changed from 944.01 nm to 1553.03 nm gradually. Then, the light spot was moved back to its initial position, and the central wavelength of the diffraction spectra were adjusted from 1553.03 nm to 944.37 nm. The displacement sensitivity and linearity were 15.310 nm/mm and 0.986, respectively. The system has a large displacement measurement range and exhibits good repeatability.

1. Introduction

In recent years, diffraction gratings have been widely used in aerospace, optoelectronic devices, biomedicine, and other fields [1–3]. The variable spacing grating (VSG) is a typical diffraction grating that can be used as a key element in displacement measurements, spectrometers, monochromators, and other systems [4–6]. Among these, displacement measurement plays an important role in automation, mechanical processing, building detection, photolithography scanners, and other engineering applications [7–10]. In particular, VSGs have become a focus of research in the field of displacement measurement owing to their anti-electromagnetic interference, fast response, compact structure, and high sensitivity [11–13], however there is still a great possibility to improve the range, sensitivity and stability of the sensing system.

Currently, optical applications based on VSG are more extensive and complete. Du et al. designed a high-spectral-resolution ultraviolet spectrograph with a wavelength range of 230–280 nm using spherical VSG [14]. Bao et al. developed a microspectrometer for VSG position sensors on an aircraft, which still have a stable output under a temperature shock environment [15]. Qian et al. proposed and demonstrated a guided-mode resonance filter with a resonant-wavelength-tunable functionality based on an VSG surface, which was fabricated using holographic interference technology [16]. Shatokhin et al. designed and implemented a scanning varied-line-spacing grating (VLSG) based spectrometer/monochromator for a wavelength range of 50-275 Å [17].

In summary, VSGs can be used in sensing systems, such as for displacement measurements. However, the operating band of a sensor system is typically in the visible range. Moreover, owing to the limitation of the grating size, the displacement measurement range is insufficient. The near-infrared band is one of the most widely studied and applied bands because of its good transmission characteristics in conventional optical fibers compared to the visible band. In this study, a large VSG was fabricated using electron beam lithography (EBL) method, and a displacement measurement system based on this VSG was designed. The system works in a wide range of near-infrared bands. Furthermore, the change in the displacement can be obtained by observing the central wavelength of the diffraction spectra.

2. Experimental setup

The diffraction principle of the VSG is shown in Fig. 1(a). The diffracted light can be produced when the incident light irradiates any position on the VSG surface. The incident light angle is θ_i, and the diffracted light is on the other side of the normal line at an angle of θ_{im}. The linewidth of the VSG is a; the line spacing is b; and the grating period is $d = a + b$. The grating line spacing increases in steps, and it remains the same for one step length and changes at the edge of the next step length. The grating line width is always fixed, and the grating period is only affected by the line spacing. The diffraction formula of VSG is given in Eq. (1), where k is the diffraction order, and λ is the central wavelength of diffracted light. When the diffraction order is $k=1$, the diffracted light angle is equal to

the incident light angle, that is $\theta_i = \theta_{im}$. If the incident light angle is sufficiently small, the diffracted light will be on the same side of the normal line as the incident light, and θ_{im} will be positive; otherwise, it will be on the other side of the normal line, and θ_{im} will be negative, as shown in Fig. 1(b). When the incident and diffracted light both lie on the same side of the normal, the optical path difference of two beams can be expressed by $d(\sin\theta_i + \sin\theta_{im}) = k\lambda$. In the experiment, the incident and diffracted light angle were fixed at 46°, and $\theta_i = \theta_{im}$. The central wavelength of the diffracted light was determined by the grating period. Therefore, displacement sensing could be achieved by observing changes in the central wavelength in the diffraction spectra.
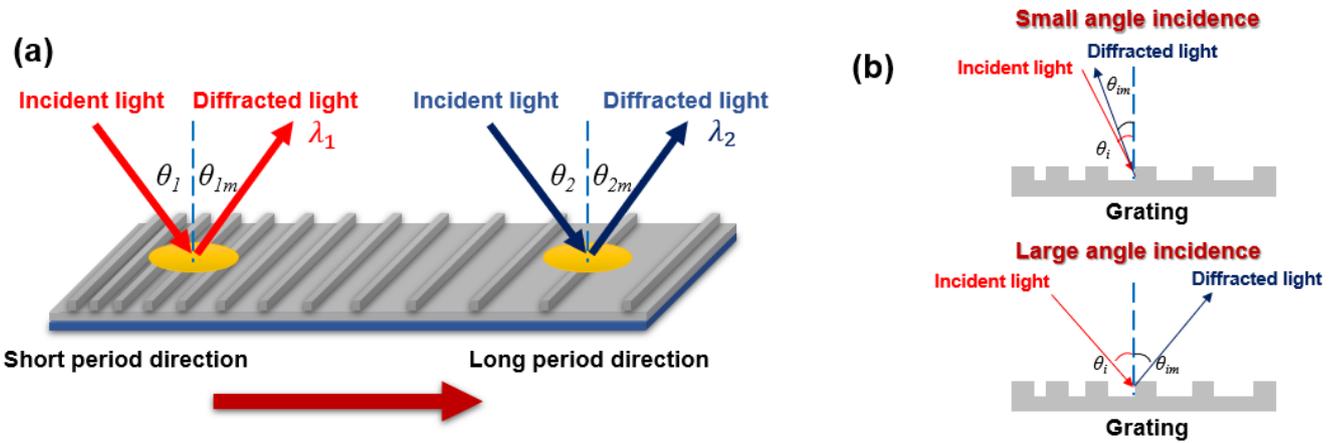
Fig. 1. Principle of proposed VSG. (a) Schematic diagram of the VSG; (b) schematic of different diffraction light angles on grating surface (color online)

$$\begin{cases} d(\sin\theta_i + \sin\theta_{im}) = k\lambda \\ d(\sin\theta_i - \sin\theta_{im}) = k\lambda \end{cases} \quad (1)$$

The displacement-sensing system was designed based on the above characteristics, and its overall structure is shown in Fig. 2. The Schematic diagram is shown in Fig. 2(a), firstly, a wideband incident light was generated by a white light source (WLS) and reached the collimator through a large-core optical fiber. The incident light was then irradiated on the surface of the VSG located on a one-dimensional displacement platform. The diffracted light was collected using another collimator and transmitted to an optical spectra analyzer (OSA) through the large-core optical fiber. The incident and diffracted light angles were adjusted using the collimator. Simultaneously, a personal computer (PC) was used to

control the one-dimensional displacement platform to move the VSG horizontally relative to the collimator. Finally, the diffraction spectra at different positions on the VSG surface were analyzed and displayed using the OSA.

The displacement sensing system built according to the sensing system diagram illustrated in Fig. 2(a) is shown in Figs. 2(b and c). The VSG was fixed on a one-dimensional displacement platform. The collimator received the incident light transmitted through the optical fiber (FIB-Y-400-L (2)-NIR, Skyray, CHN) generated by the WLS (SLS201L, Thorlabs, US), and its angle was adjusted using an angle disk, the collimator (F220SMA-A) NA is 0.25, and focal length is 10.92 mm. Finally, the OSA (600-1700 nm, AQ6370C, YOKOGAWA, JPN) showed the diffraction spectra of the VSG.
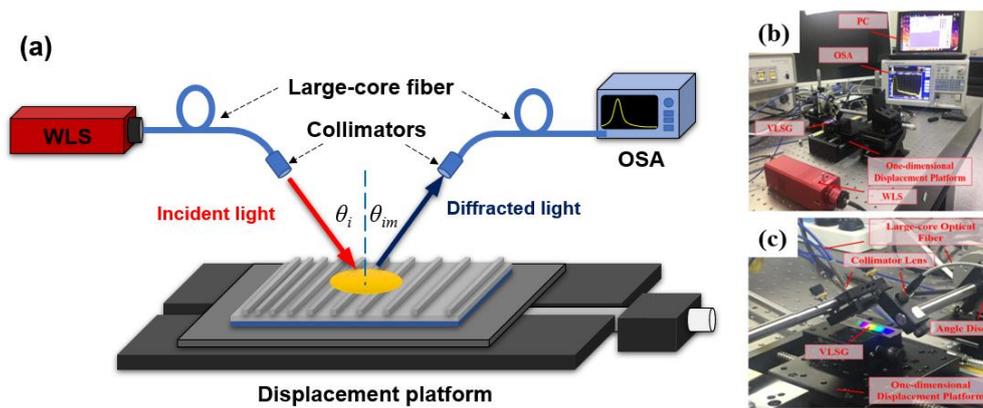
Fig. 2. The proposed displacement sensing system. (a) Schematic of displacement sensing system based on VSG; (b) overall structure   of the experimental system and (c) VSG on a one-dimensional displacement platform (color online)

The displacement sensor was tested using the system shown in Fig. 2, and the angles of the two collimators were fixed throughout the experiment. The VSG was moved horizontally by the displacement platform to change the position of the light spot formed by the incident light irradiating on the VSG surface. The light spot was moved from a position with high line density to a position with low line density. As the line density decreased (the grating period increased), the central wavelength of the diffraction spectrum collected by the OSA increased. The displacement of the VSG was obtained by observing the change in wavelength. Moreover, the repeatability of the sensor system was verified by returning the spot to its initial position.

3. Experimental results and discussion

The proposed grating was based on a quartz plate, which exhibits excellent thermal shock stability. Before the grating was inscribed by EBL technique, the grating substrate was cleaned and coated with an aluminum layer and a photoresist. The quartz plate was placed in an EBPG

5000 Plus electron beam exposure machine, and the effective writing field was 260 μm × 260 μm, which satisfied the experimental requirements. The exposure dose used in the processing was 245 uC/cm^3, and the electron beam acceleration voltage was 100-kV. During the writing process, the position of the writing field and exposure pattern were controlled using an electronic deflector. Fig. 3 shows a schematic of the EBL manufacturing grating structure. After the exposure process, the quartz plate was developed in an AR 300-47 developing solution; the grating structure was fixed on the photoresist; and the aluminum layer was etched using the reactive ion etching (RIE) method. Finally, the VSG was coated with aluminum film, and then cleaned with isopropyl alcohol, and the quartz substrate was sliced to complete the fabrication process. The VSG is shown in Fig. 3. The grating region size of the VSG was 80 mm × 10 mm. Specifically, the maximum and minimum line densities of the grating were 950 L/mm and 400 L/mm, respectively. For the proposed grating inscription method, it was possible to fabricate larger size grating through combining different gratings.
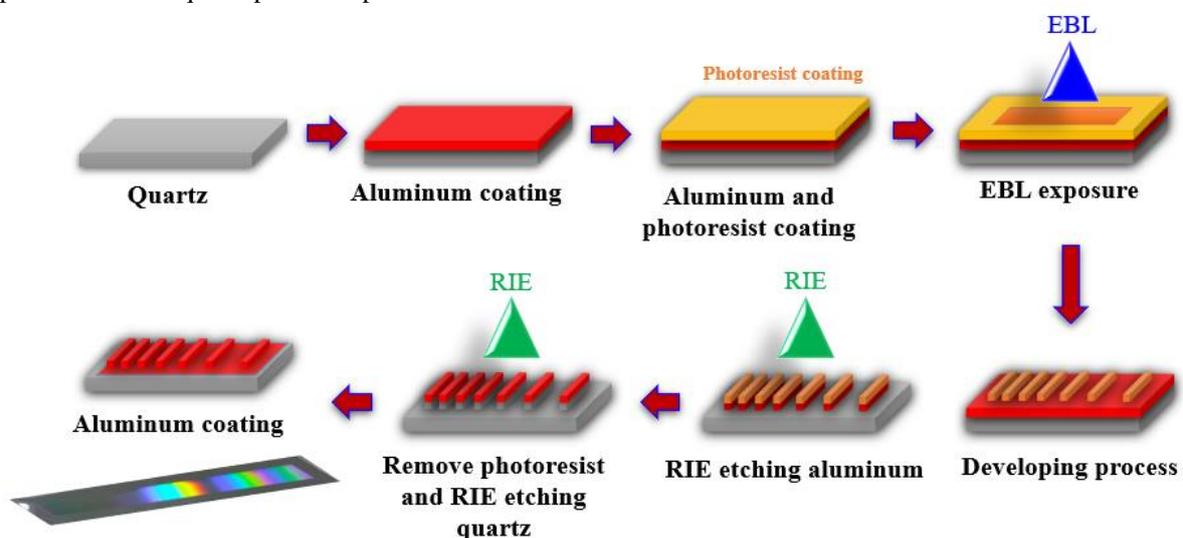
Fig. 3. Schematic of electron beam exposure manufacturing grating structure (color online)

First, a displacement experiment of the light spot toward the direction with a large period was conducted. The two collimators were adjusted such that the incident and diffracted light angles were fixed at 46°. The light spot was moved to the end with the highest VSG line density, and the one-dimensional displacement platform was controlled to make the VSG move 40 mm horizontally to the direction with the lower line density, and the displacement interval was 5 mm. The changes in the diffraction spectra when the light spot was at different positions are shown in Fig. 4(a). The central wavelength of the diffraction spectrum increases from 944.01 nm to 1553.03 nm as the increase of grating period in the light spot irradiation area. The variation in the central wavelength of the diffraction spectra is shown in Fig. 4(b). Each point in the figure represents the central wavelength of the diffraction spectra for different displacements. Through linear fitting of each point, the displacement sensitivity was found to be 15.138 nm/mm, and the linearity was 0.986, the displacement measurement

has excellent linearity. The results show that the displacement sensing system had high displacement sensitivity. The linear relationship between grating period and central wavelength of diffraction spectrum was also confirmed. This was because the incident and diffracted light angles were unchanged, and the central wavelength of the diffraction spectra was only affected by the grating period. The variation trends of the peak output power and the 3-dB bandwidth of the diffraction spectra are shown in Figs. 4(c) and (d), respectively. With an increase in the grating period, the output power of the diffraction spectra tended to decrease, whereas the bandwidth gradually increased. This was because when the grating surface period is large, its diffraction efficiency will gradually decrease, leading to a decrease in the power of the diffracted light. And the intensity of the diffracted light received by the collimator changes with the movement of the grating, which also affects the optical power to some extent.
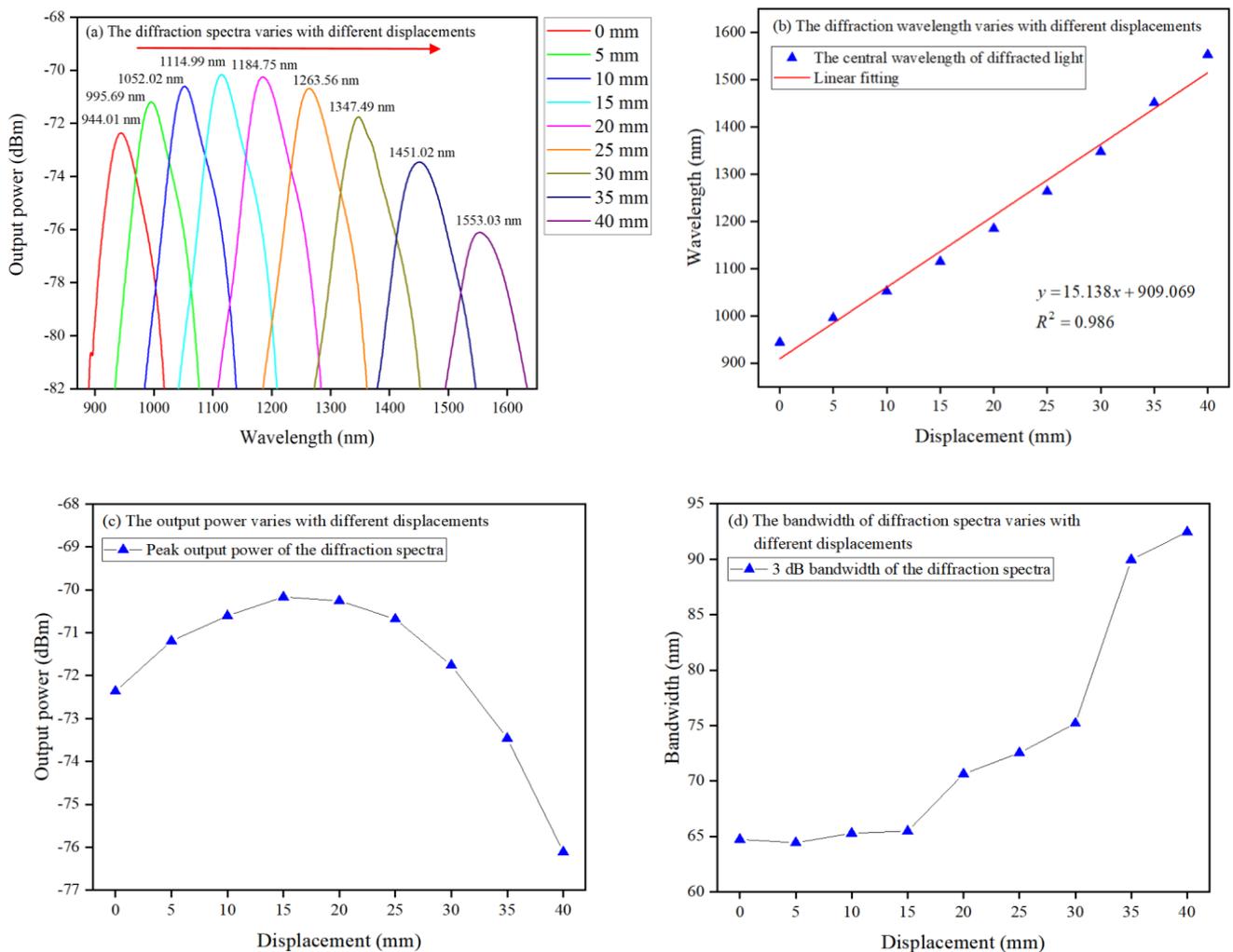
Fig. 4. Displacement experiment of the light spot toward the direction with a large period: (a) shift of the diffraction spectra, (b) variation in the central wavelength, (c) variation in the output power, and (d) variation in the bandwidth (color online)

The angle of the collimator remained unchanged. The light spot was moved back to its initial position using the one-dimensional displacement platform. The total displacement was still 40 mm, and the displacement interval was 5 mm. The changes in the diffraction spectra when the light spot was at different positions are shown in Fig. 5(a). With the decrease of grating period, the diffraction wavelength decreases from 1553.02 nm to 944.37 nm. The variation in the central wavelength of the diffraction spectra is shown in Fig. 5(b). Based on the linear fitting of each point, the displacement sensitivity was 15.130 nm/mm, and the linearity was 0.986. This result is similar to the experimental result shown in Fig. 4(b). The variation trends of the peak output power and the 3-dB bandwidth of the diffraction spectra are shown in Figs. 5(c) and 5(d), respectively. With a decrease in the grating period,

the output power of the diffraction spectra tended to increase, whereas the bandwidth gradually decreased. As mentioned earlier, the system exhibited good displacement sensitivity and linearity for the light spot traveling along the same path. When the incident light spot irradiates at different splicing grating positions, the diffracted light wavelength is generated according to different line widths grating. For the proposed grating, the diffracted light loss was increased seriously as light spot was changed to the larger range more than 40 mm. The bandwidth trends shown in Figs. 4(d) and 5(d) were not linear, because of error of grating fabrication procedure. The grating was inscribed through EBL and IRE step; thus, the error was generated gradually. In the next step, the inscription process will be optimized to improve grating sensing capability.
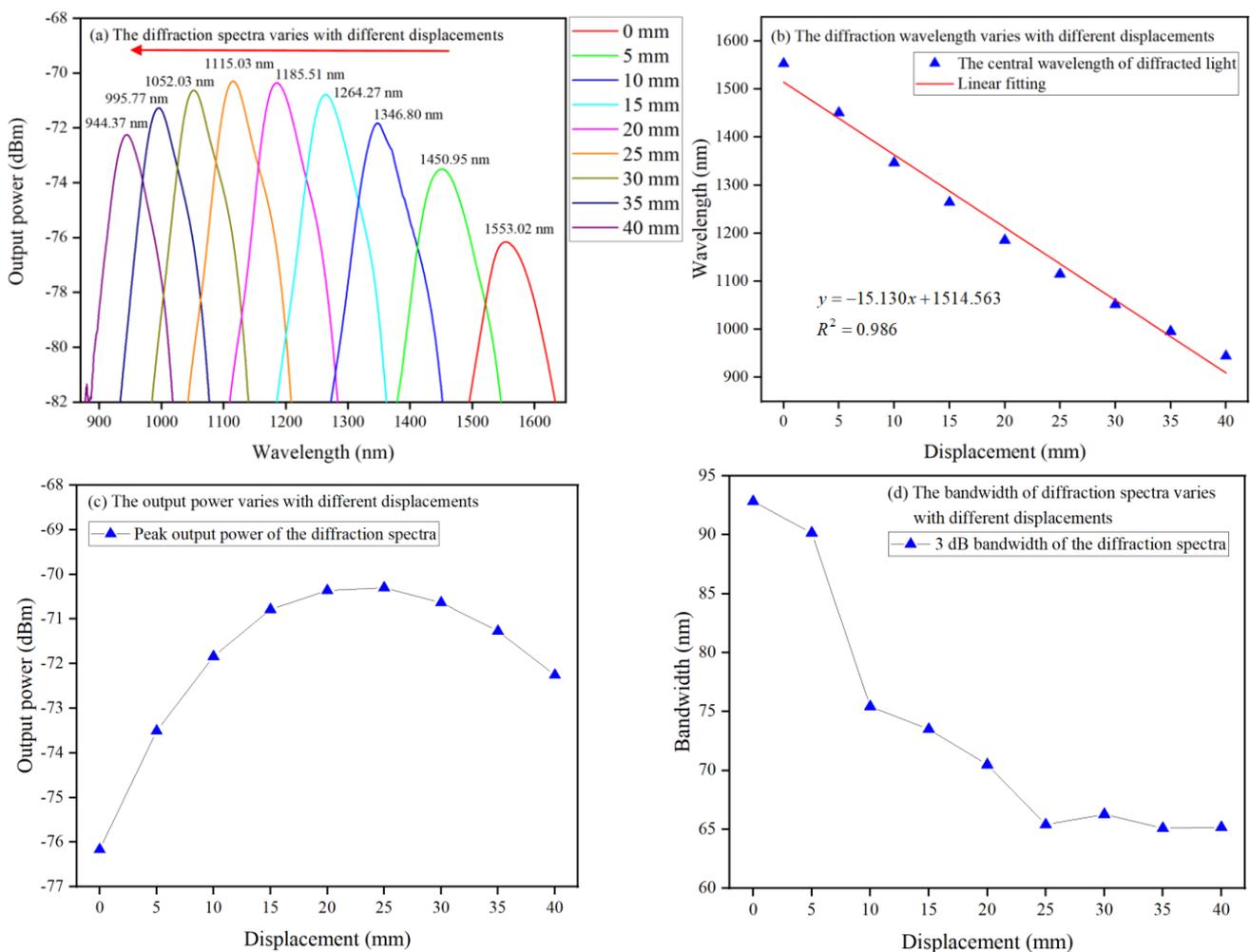
Fig. 5. Displacement experiment with the light spot moving in the direction of the small period: (a) shift of the diffraction spectra, (b) variation in the central wavelength, (c) variation in the output power, and (d) variation in the bandwidth (color online)

Finally, the repeatability of the displacement sensing system was verified based on the experimental results shown in Fig. 6 shows the variation in the central wavelength of the diffraction spectra for the entire travel distance of the light spot on the VSG surface. The x-axis

represents the distance between the light spot and end of the maximum line density of the VSG. Regardless of an increase or decrease in the grating periods, the central wavelengths of the diffraction spectra corresponding to the same grating periods were identical, with a maximum

difference of 0.76 nm. The small error was due to the displacement accuracy of the one-dimensional displacement platform. Therefore, the displacement - sensing system exhibited good repeatability.
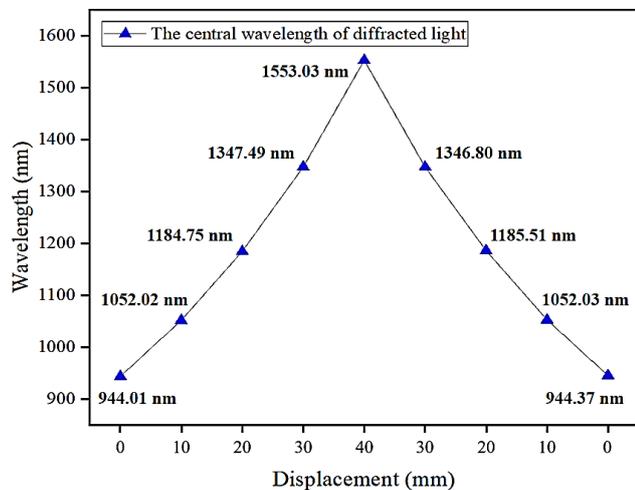
Fig. 6. Repeatability test results of displacement sensing system

4. Conclusions

In this study, a displacement sensing system based on a reflective varied-line spacing grating was designed. The grating area was 80 mm × 10 mm, and an VSG was fabricated using electron beam lithography. The incident and diffraction light angles were fixed at 46°. The experimental results showed that the central wavelength of the diffraction spectra changed from 944.01 nm to 1553.03 nm as the VSG moved 40 mm horizontally towards the large-period direction. Then, the VSG was moved back to its original position, and the central wavelength of the diffraction spectra changed from 1553.03 nm to 944.37 nm. The displacement sensitivities were 15.318 and 15.310 nm/mm, respectively. The displacement sensing system has two collimators to transmit incident light and diffracted light, which has good linearity, good repeatability and compact structure. The developed system can satisfy large range accurate displacement measurement in the near infrared band range, and the grating structure can be extended to achieve composite multi-parameter sensing, which has great potential in aircraft, robotics and other applications.

References

[1] D. M. Miles, J. A. Mccoy, R. L. Mcentaffer, C. M. Eichfeld, G. Lavallee, M. Labella, W. Drawl, B. Liu, C. T. Deroo, T. Steiner, Astrophysical Journal **869**, 95 (2018).
[2] C. Hou, Z. Y. Li, C. F. Zhou, X. L. Zhang, L. Ye, Z. Yang, W. Zhang, L. Li, P. P. Xu, P. Q. Zhang, T. F. Xu, Infrared Physics & Technology **127**, 104379 (2022).
[3] Y. Y. Li, Q. Q. Chen, B. Wu, L. L. Shi, P. Tang, G. Z. Du, G. Q. Liu, Results in Physics **15**, 102760 (2019).
[4] Z. G. Lu, P. P. Wei, C. Q. Wang, J. L. Jing, J. B. Tan, X. P. Zhao, Measurement Science & Technology **27**, 074012 (2016).
[5] J. W. Chen, W. Chen, G. D. Zhang, H. Lin, S. C. Chen, Optics Express **25**(11), 12446 (2019).
[6] C. F. Xue, Y. Q. Wu, Y. Zhou, L. Xue, Y. Wang, Z. Xu, R. Tai, Journal of Synchrotron Radiation **22**, 328 (2015).
[7] N. Zhao, G. Qian, X. C. Fu, L. J. Zhang, W. Hu, R. Z. Li, T. Zhang, Optical Engineering **56**(2), 027109 (2017).
[8] S. Donati, M. Norgia, Optical Engineering **57**(5), 051506 (2018).
[9] A. B. Klemm, D. Stellinga, E. R. Martins, L. Lewis, L. O. Faolain, T. F. Krauss, Optical Engineering **53**(9), 095104 (2014).
[10] W. T. Zhang, Y. L. Wang, H. Du, Q. L. Zeng, X. M. Xiong, Optical Engineering **59**(4), 045101 (2020).
[11] L. Long, Z. Guo, S. Zhong, IEEE Sensors Journal **19**, 2880784 (2018).
[12] B. Wang, H. T. Li, W. H. Shu, W. H. Li, L. Chen, L. Lei, J. Y. Zhou, Modern Physics Letters B **30**(1), 1550257 (2016).
[13] E. A. Vishnyakov, A. O. Kolesnikov, A. S. Pirozhkov, E. N. Ragozin, A. N. Shatokhin, Quantum Electronics **48**(10), 916 (2018).
[14] L. L. Du, X. W. Du, C. Y. Li, N. An, Q. P. Wang, Spectroscopy and Spectral Analysis **35**(6), 1751 (2015).
[15] J. G. Bao, Z. K. Liu, H. Y. Chen, J. P. Lin, S. J. Fu, Spectroscopy and Spectral Analysis **35**(5), 1409 (2015).
[16] L. Y. Qian, K. N. Wang, C. Q. Han, IEEE Photonics Technology Letters **29**(11), 925 (2017).
[17] A. O. Kolesnikov, E. A. Vishnyakov, A. N. Shatokhin, E. N. Ragozin, Quantum Electronics **49**(11), 1054 (2019).

---
[*]Corresponding author: gregg1986@sina.com
                            tanqimeng@foxmail.com